Ultrasound in Med. & Biol., Vol. 44, No. 8, pp. 1873–1881, 2018

0301-5629/$ - see front matter

https://doi.org/10.1016/j.ultrasmedbio.2018.04.001

● *Original Contribution*

VALIDATION OF AN OPEN-SOURCE TOOL FOR MEASURING CAROTID LUMEN DIAMETER AND INTIMA–MEDIA THICKNESS

Hugo Luis Manterola,*,† Lucas Lo Vercio,*,† Alejandro Díaz,† Mariana del Fresno,*,‡ and Ignacio Larrabide*,†

* Pladema Institute, Universidad Nacional del Centro de la Provincia de Buenos Aires, Tandil, Argentina; † Consejo Nacional de Investigaciones Científicas y Técnicas (CONICET), Buenos Aires, Argentina; and ‡ Comisión de Investigaciones Científicas de la Provincia de Buenos Aires (CICPBA), Buenos Aires, Argentina

(*Received* 10 *November* 2017; *revised* 20 *February* 2018; *in final form* 2 *April* 2018)

Abstract—In low- and middle-income regions, a relatively large number of deaths occur from cardiovascular disease or stroke. Carotid intima–media thickness (cIMT) and carotid lumen diameter (cLD) are strong indicators of cardiovascular event risk and stenosis severity, respectively. The interactive open-source software described here, Cimtool, is based on active contours for measuring these indicators in clinical practice and thus helping in preventive diagnosis and treatment. Cimtool was validated using carotid phantoms and real images obtained using ultrasound. Expert users measured cIMT and cLD in regular practice and also with Cimtool. The results obtained with Cimtool were then compared with the results for the manual approach in terms of measurement agreement, time spent on the measurements and usability. Intra-observer variability when using Cimtool was also analyzed. Statistical analysis revealed strong agreement between the manual method and Cimtool ($p > 0.01$ for cIMT and cLD). The correlation coefficient for both cIMT and cLD measurements was $r > 0.9$. Moreover, this software allowed the users to spend considerably less time on each measurement (3.5 min per study versus 50 s with Cimtool on average). An open-source, interactive, validated tool for measuring cIMT and cLD clinically was thus developed. Compared with the manual approach, Cimtool's straightforward measurement flow allows the user to spend less time per measurement and has less standard deviation. The coefficients of variation for measurements and intra-observer variability were lower than those reported for recent automated approaches, even with low-quality images. (E-mail: manterolaluis@conicet.gov.ar) **© 2018 World Federation for Ultrasound in Medicine & Biology. All rights reserved.**

Key Words: **Carotid, Lumen diameter, Intima–media thickness, Ultrasound, Measurement tool, Active contours.**

INTRODUCTION

Motivation

Cardiovascular diseases (CVDs) are one of the leading causes of disability and morbidity worldwide. Recent reports indicate that around 16 million people have a stroke every year. Additionally, these afflictions combined cause more deaths than any other, with 8 million caused by CVDs and 7 million caused by stroke (World Health Organization [WHO 2016). Furthermore, a significant percentage (~70%) of these deaths occur in low- and middle-income populations (Avezum et al. 2009; World Health Organization (WHO 2014).

Carotid artery disease is a primary example of CVD and is caused by atherosclerosis (Araki et al. 2014). Atherosclerosis is a progressive process consisting of the growth of lipid plaques that damage the endothelium of the arteries. This accumulation narrows the lumen, blocking the flow of blood and oxygen (Sobieszczyk and Beckman 2006). As the disease progresses, the plaque can break up, resulting in emboli flowing downstream from the affected location, in turn leading to a stroke or myocardial infarction. Therefore, carotid lumen diameter (cLD) is considered a strong biomarker for stenosis assessment (Araki et al. 2016). Additionally, carotid intima–media thickness (cIMT) is another well-established indicator for monitoring CVD and predicting the occurrence of major adverse cardiovascular events (Polak et al. 2010). Several studies have reported threshold cIMT values that indicate the presence of cardiovascular disease when exceeded (Araki et al. 2015; Ikeda et al. 2013). Recent works have

Address correspondence to: Hugo Luis Manterola, Pladema Institute, Universidad Nacional del Centro de la Provincia de Buenos Aires, Gral Pinto 399, Tandil, Argentina. E-mail: manterolaluis@conicet.gov.ar

Conflicts of Interest: The authors declare that there are no conflicts of interest in this work.

also revealed a strong relationship between cIMT values and the severity of coronary artery disease (Golemati et al. 2007; Ikeda et al. 2015). Thus, it has been determined that cIMT and cLD are strong, independent risk biomarkers of significant interest for predicting and diagnosing cardiovascular events.

B-Mode ultrasound (US) imaging is a non-invasive, real-time and relatively inexpensive technique widely used for the visualization and measurement of cLD and cIMT (Shung 2015).

Previous works

On the one hand, manual measurements are tedious and have higher intra-observer variability Molinari et al. (2010). Consequently, reliability, accuracy, reproducibility and monitoring of the measures could be compromised, because measurements are taken at a limited number of points along the interface of the carotid (McCloskey et al. 2014). In this regard, several studies have discussed the need for systems for carotid measurement computation (Bots et al. 2007; Polak et al. 2010; Pursnani et al. 2014). On the other hand, automated image-based identification of the carotid tissue is very challenging (Molinari et al. 2010). Several aspects such as transducer frequency and type, scanning protocol, orientation of the probe, control gain, zooming and quality of the embedded software greatly hinder that task (Bastida-Jumilla et al. 2013; Nicolaides et al. 2011; Saba et al. 2014; Sanchez et al. 2012). Furthermore, plaque growth at the interface of lumen and tunicas could create variations in image contrast depending on its composition (Suri et al. 2005). In the presence of poor image quality, interactive tools are mandatory to correct errors because fully automated tools fail when blood backscattering or side vessel shadows artifacts are present (Delsanto et al. 2007).

Our approach

Considering all previous premises, we have developed, assessed and made available online an open-source, interactive tool called Cimtool for assisting physicians in the assessment of both cLD and cIMT. An adequate compromise between (i) accuracy and reliability compared with sonographer's manual readings and (ii) robustness when using low-quality or heterogeneous images was pursued. Carotid phantoms were previously developed (Manterola et al. 2017). These were imaged using a regular ultrasound machine for a first assessment of our system. Then, images from real patients with plaque, artifacts and different levels of zooming were used. On our set of images, two expert users of carotid ultrasound imaging measured cLD and cIMT both manually and using Cimtool. Additionally, Cimtool intra-observer variability and time spent with each measurement method was analyzed.

METHODS

Development of Cimtool

Cimtool was developed using specialist software (MATLAB, The MathWorks, Natick, MA, USA). Its architecture is schematically represented in Figure 1. The workflow is the same whether cLD or cIMT is to be measured, and it was developed to be simpler than the manual approach without compromising accuracy. Measurement methodology described in Wikstrand (2011) was followed. First, a DICOM image provided by the ultrasound machine must be loaded. After that, at least one point has to be placed near the near lumen–intima interface when measuring cLD or the far lumen–intima interface when measuring cIMT. Normally, the more blurry or noisy is the interface, the more points are required. After the user

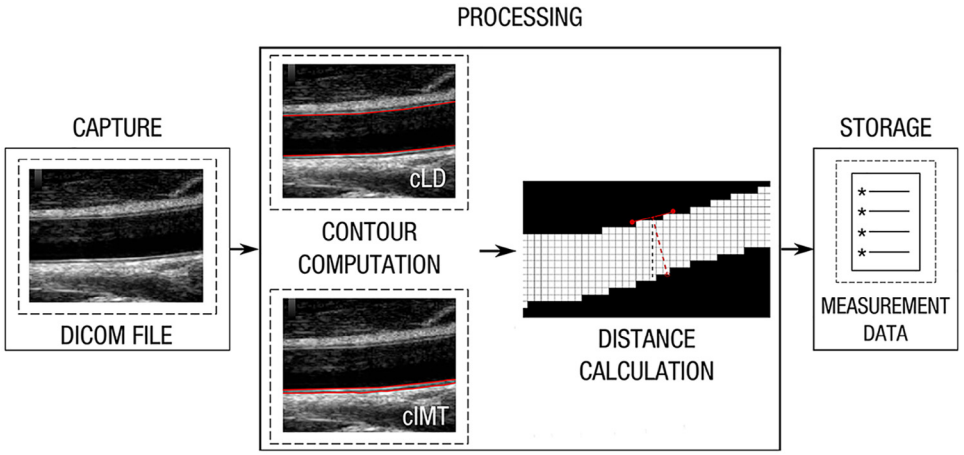

Fig. 1. High-level schematic view of Cimtool. Contours over interfaces of interest are computed on a DICOM carotid image. Measurements and statistics are then stored. cIMT = carotid intima–media thickness; cLD = carotid lumen diameter.

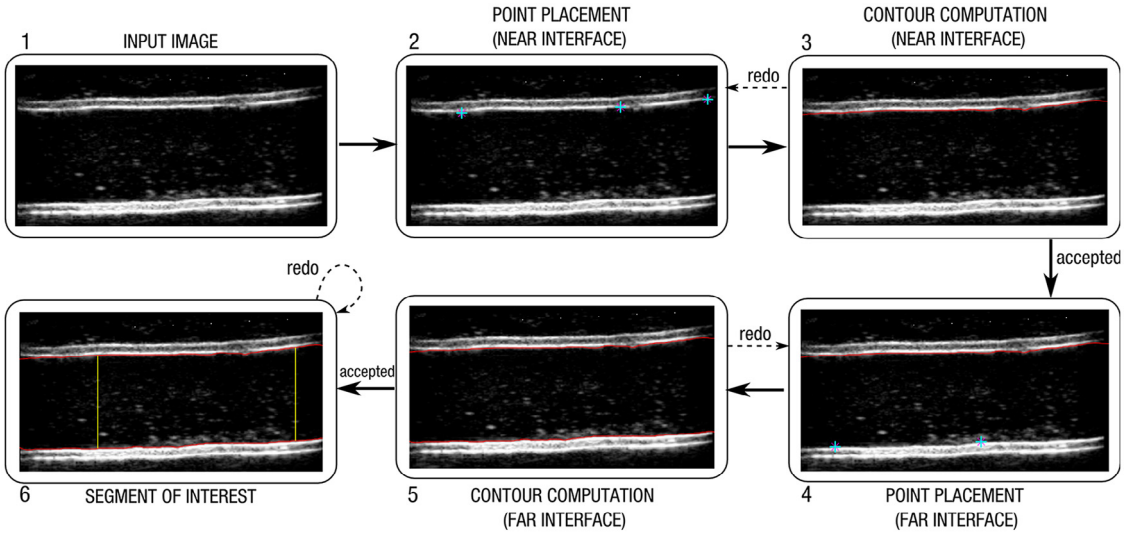

Fig. 2. Cimtool workflow for calculation of carotid lumen diameter. The process for measurement of carotid intima–media thickness is analogous. (a) Image is loaded. (b) Points are placed over near lumen–intima interface. (c) Contour for near lumen–intima interface is calculated. If the contour is not satisfactory, it can be re-calculated without re-starting the entire process. (d) Points are placed over far lumen–intima interface. (e) Contour for far lumen–intima interface is calculated. (f) Segment of interest is chosen.

completes placement of the points, a contour is calculated and drawn over the image as explained in the following section. If the contour is unsatisfactory to the user, it can be re-calculated without re-starting the process. In the next step, the user indicates points on the far lumen–intima interface (cLD) or far media adventitia (cIMT), where another contour is calculated and drawn. After both contours are accepted, the user must select a segment of interest for measurement by clicking on the segment's beginning and end. Finally, two files are stored: one containing measurement statistics such as average, median, mean and standard deviation and another containing the chosen point coordinates, the nodes of the contour and the distances between those nodes (*i.e.,* the measurements as detailed below). A scheme of this workflow is provided in Figure 2, for the case of cLD measurement; for cIMT measurement, the workflow is analogous.

Contour deformable model

Active contours have been widely used for medical image processing and specifically for cIMT identification (Bastida-Jumilla et al. 2015; McInerney and Terzopoulos 1996; Molinari et al. 2010). They provide an extensible framework for detecting objects with blurry boundaries in noisy images, such as in the present study. The active contour model consists of a parametric closed curve of N nodes. Based on an initial contour, the location of each node of the curve X moves iteratively according to the first-order ordinary differential equation of motion. The equation to update node X_i from iteration i to $i + 1$ is

$$X_{i+1} = X_i - \frac{1}{\gamma}\left(a\alpha_i + b\beta_i - q\rho_i - pf_i\right) \quad (1)$$

where α_i, β_i, ρ_i and f_i are the stretching force, bending force, inflation and edge attraction at X_i, respectively. Equation (1) iteratively proceeds until the displacement of every node does not exceed a given error tolerance (*i.e.,* $X_{i+1} \sim X_i$).

To use this framework in the present problem, some adaptations were required. In a long-axis view of a carotid artery, a contour representing the edge of a wall is not a closed curve. A direct application of the deformable model would generate an imbalance in the forces affecting the first and last nodes, being propagated through the iterations. This will lead to the curve curling over itself over the boundaries of I. On the other hand, To solve this, the image I is extended to right and left (I_{ext}) with a matrix of zeros of arbitrary width. When the deformation of the curve stops, the nodes of the curve located in the added regions are discarded.

For stretching and bending forces, some adaptations were done as well. As the user places points close to the edge of interest, the force ρ_i can be disregarded, leaving the edge attraction f_i as the only external force. Furthermore, as no *a priori* information on concavity or convexity of contours could be assumed, the bending force β_i must be set to 0. Then, eqn (1) is re-written as

$$X_{i+1} = X_i - \frac{1}{\gamma}\left(a\alpha_i - pf_i\right) \quad (2)$$

To compute f_i, I_{ext} was first filtered using a median filter with a 3×3 window. This filter is useful for general

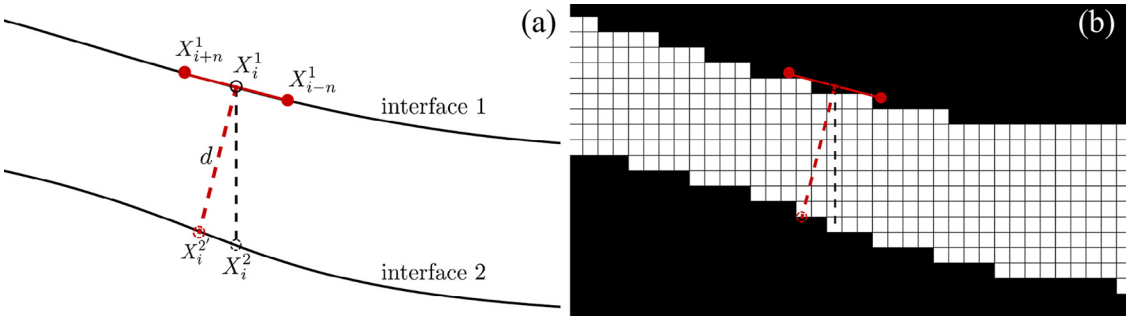

Fig. 3. Distance computation. (a) X_i^1 is the current node on interface 1, and X_{i+1}^1 and X_{i-1}^1 are the nodes used to calculate the perpendicular node X_i^2 on interface 2 to compute d, which is the correct distance between the curves. The *black dashed line* indicates the distance if the column corresponding to X_i^1 is used. (b) Binary mask with the calculation at the pixel level.

despeckling purposes (Lo Vercio et al. 2016). Then, a gaussian gradient G_σ filter is applied. Because of the horizontal disposition of the edges (*i.e.,* artery walls),

$$f_i = \frac{\partial}{\partial_y}\left|\frac{\partial}{\partial_y}(G_\sigma * I_{ext})\right|$$

The values $\gamma = 10$, $a = 0.15$, $p = 1$ and $\sigma = 0.3$ were experimentally determined and used in our experiments.

Contour distance

As lumen–intima, intima–media and media–adventitia interfaces are relatively parallel and horizontally disposed, computing the distance between two nodes of the curves by counting the number of pixels in their columns seems a natural choice. However, as these interfaces are irregular, considering two nodes in the same column might not be an accurate representation (Fig. 3). For this reason, the closest point was obtained by searching in the perpendicular direction. As illustrated in Figure 3(a), from the node X_i in interface 1, two nodes X_{i-n} and X_{i+n} are selected. A straight segment S intersecting X_{i-n} and X_{i+n} is computed, and then a perpendicular segment to S directed toward interface 2 is retrieved.

To compute the actual distance, a mask of the image I is created, setting to 1 all the pixels between the interfaces and setting to 0 the rest (Fig. 3b). Starting on X_i^1, an iterative process starts in the direction of the perpendicular slope. By use of subpixel steps, the process stops when a zero value is found. Then, the Euclidean distance between X_i^1 and X_i^2 is computed. It is worth mentioning that the real size of a pixel is obtained from the DICOM image provided by the ultrasound machine.

This process is repeated for all the nodes in the curve corresponding to interface 1, resulting in a set of measurements. Then, the mask is flipped and a new set of measurements are obtained in the same way. The final measurements are calculated by averaging these two sets. Finally, mean, median and standard deviation are computed.

Experimental setup

Carotid phantoms. We developed phantoms to assess the viability of the tool for measuring cLD and cIMT. These were made with layers of gelatin and porcine meat that resembled a carotid artery when subjected to ultrasound analysis. Further details on the development of these phantoms can be found in Manterola et al. (2017). Ultrasound images of the phantoms were taken using a compact console ultrasound system (Esaote MyLab40, Esaote Group, Genova, Italy) with linear transducer LA523, as illustrated in Figure 4. Cimtool was also tested on ultrasound images of real carotid arteries taken with the same equipment.

Validation. Fifteen ultrasound images of a single carotid phantom and 70 images of the common carotid arteries of patients were analyzed separately. Fifty-five percent of the patients were male; the age range was 15–55 yrs. All patients were examined as in a routine checkup. The protocol for this research was evaluated and approved by the institutional ethics and research committee. The study was carried on in agreement with the Declaration of Helsinki and the Guideline for Good Clinical Practice of the European Medicines Agency. Written informed consent was obtained from the participants or their responsible person. For each image, a segment of interest 2.5 cm wide or larger was considered. For cIMT measurements in particular, Cimtool checks that a minimum of 150 points (*i.e.,* active contour nodes) can be computed in the selected region, according to the Manheim Consensus (Touboul et al. 2012). Then, cIMT and cLD were manually calculated according to the normal practice (Fig. 4). Expert users placed 15 points per interface and averaged manually the distances between them for every image (Fig. 5). The same indicators were then mea-

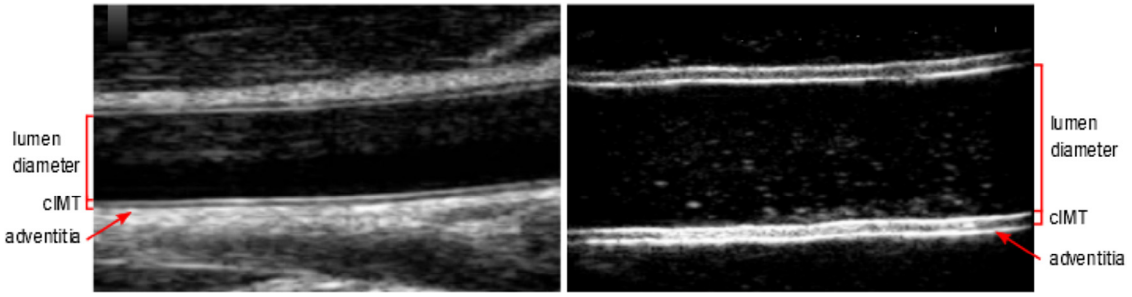

Fig. 4. Left: Real carotid image revealing the measurements of interest in this study. Right: Analogous carotid phantom ultrasound image revealing the same measurements.

sured using Cimtool. Measurements with Cimtool were performed twice to assess intra-observer variability.

Both for the manual method and Cimtool, measurements from an image I are blocks of data (*i.e.,* distances between the caliper points or the nodes of the contours, respectively). For every image along a region of interest ≥2.5 cm, n_1 distances were computed for the manual approach and n_2 distances for Cimtool ($n_1 << n_2$). Caliper points in the manual measurements and nodes in Cimtool do not correspond one to one.

To determine the appropriate statistical test to be used on the data, two aspects were assessed: (i) the normality of the residuals and (ii) the homoscedasticity *(i.e.,* the homogeneity of the variances). It is important to note that if (i) and (ii) are not true, statistical tests cannot be assumed to be valid. For (i), a Shapiro–Wilk test was carried out. The null hypothesis of this test is that the residuals' distribution of the measurements is normal. For (ii), a variance test $F = S_1/S_2$ with $N_a - 1$ and $N_m - 1$ degrees of freedom ($N_a = 12750$ and $N_m = 1275$) was performed. The null hypothesis in this case is that the variances are homogeneous. Both phantoms and real images measurements presented homoscedasticity and not normality of the residuals, which are the pre-conditions for applying a non-parametric analysis of variance (ANOVA) test such as Kruska–Wallis. This test was then carried out to detect statistically significant differences between measurements.

Additionally, the expert users measured each image twice when using Cimtool so that intra-observer reliability could be evaluated. An ANOVA test was performed comparing both sets of measurements for each indicator (cIMT and cLD). Also, the time spent on measuring cLD and cIMT with both methods was recorded.

RESULTS

Statistical validation

Normality of the residuals was determined using the Shapiro–Wilk test. The null hypothesis was rejected ($p < 0.01$) for cLD and cIMT in both cases (phantoms and real images).

Homoscedasticity was determined using the variance test $F = S_1/S_2$. The null hypothesis was accepted with $p > 0.01$ for cLD and cIMT in both cases (phantoms and real images).

Provided homoscedasticity and non-normality of the residuals, a non-parametric ANOVA (Kruskal–Wallis) test was used. The test revealed that there are no statistically significant differences between the measurement methods (see Table 1). Bland–Altman plots revealed a mean cIMT difference of -0.02 ± 0.03 and a cLD difference of -0.03 ± 0.19 (Fig. 6). The correlation coefficient $r^2 > 0.9$ was obtained for both cIMT and cLD measurements.

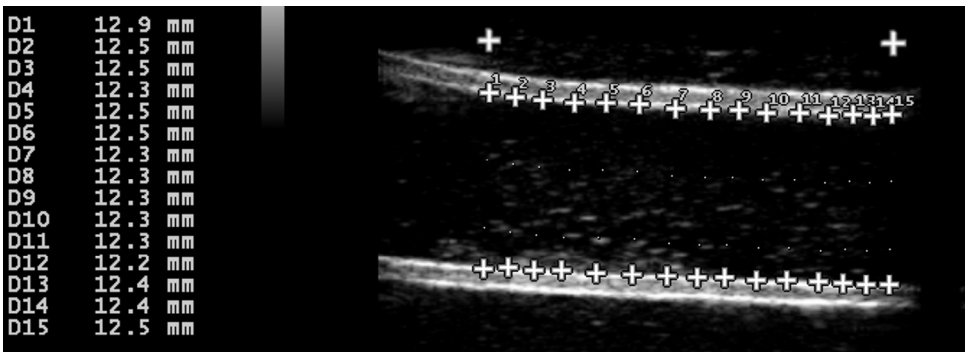

Fig. 5. Manual approach using Esaote MyLab40 for carotid lumen diameter measurement. The cardiologist placed as many caliper points as possible inside the region of interest and then manually averaged the distances between corresponding points.

Table 1. Kruskal–Wallis test of cLD and cIMT calculations*

Case	Type	n	Mean	SD	Median	$p^{\dagger}$
cIMT						
Phantom	Manual	225	1.30 mm	0.16 mm	1.30 mm	0.21
	Cimtool	2250	1.29 mm	0.11 mm	1.22 mm	
Real	Manual	1050	0.62 mm	0.06 mm	0.56 mm	0.26
	Cimtool	10,500	0.59 mm	0.02 mm	0.52 mm	
cLD						
Phantom	Manual	225	11.94 mm	0.31 mm	12 mm	0.36
	Cimtool	2250	11.99 mm	0.26 mm	12.03 mm	
Real	Manual	1050	5.9 mm	0.56 mm	6.1 mm	0.4
	Cimtool	10,500	5.65 mm	0.46 mm	5.7 mm	

cIMT = carotid intima–media thickness; cLD = lumen diameter; SD = standard deviation.
* Number of distances considered for each approach.
† p values > 0.01 indicate that there is no statistically significant difference between the manual and Cimtool measurements for either case.

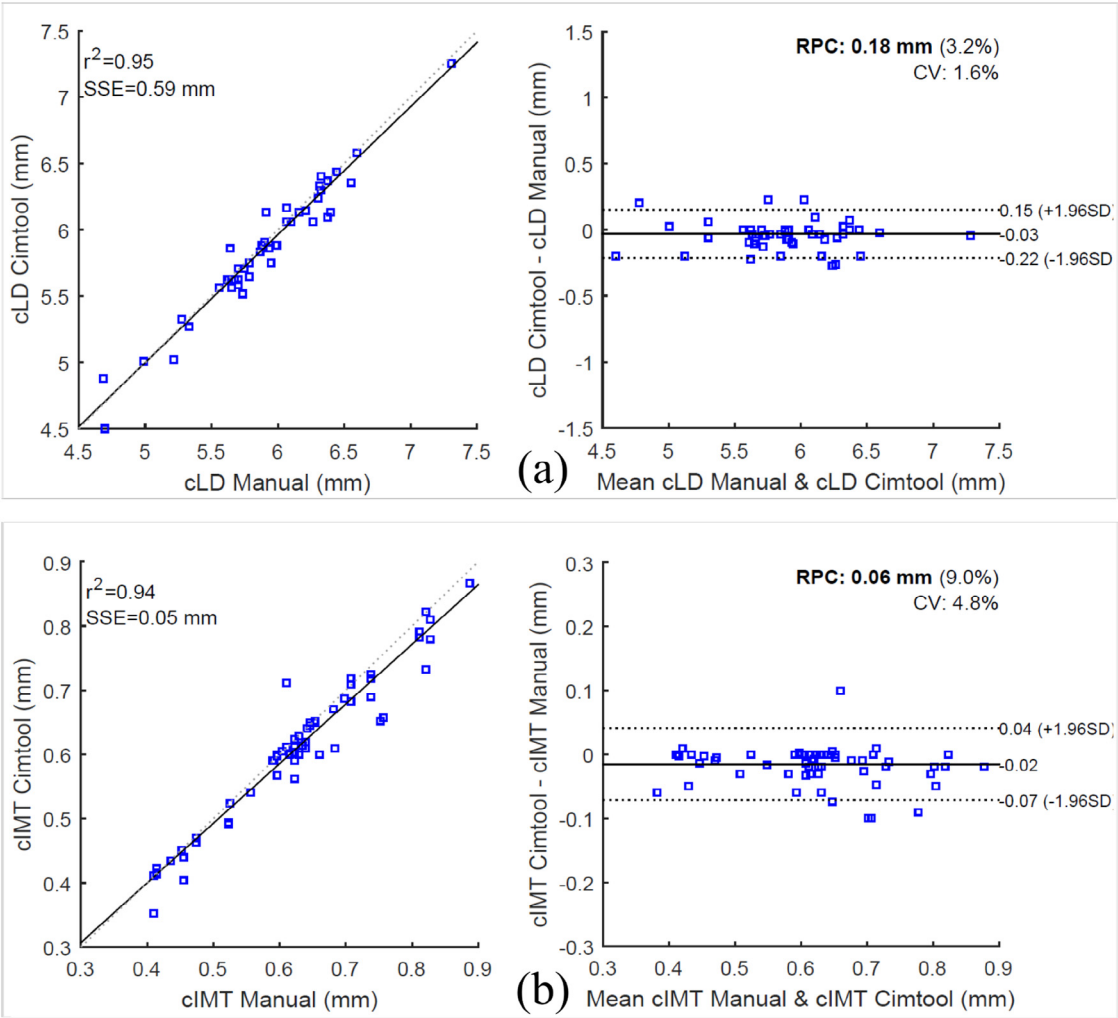

Fig. 6. Bland–Altman and correlation plots. Each point in the plots corresponds to the mean cLD and cIMT measured for an image. (a) cIMT measurements. (b) cLD measurements. cIMT = carotid intima–media thickness; cLD = carotid lumen diameter; CV = coefficient of variation; RPC = reproducibility coefficient; SD = standard deviation; SSE = sum of squared errors of prediction.

Table 2. Qualitative aspects*

Type	Points placed	Computed distance	Time per image	SD
Manual	5100	2550	3.5 min	0.6 min
Cimtool	809	12,750	0.9 min	0.2 min

SD = standard deviation.

* Users placed 5100 caliper points for manual measurements and 809 for measurements using Cimtool (30 and 9.5 points per image, respectively). Experts spent 3.5 min per image for the manual approach and 0.9 min per image with the tool, on average. Cimtool computed 12,750 distances, and the manual approach computed 2550 distances.

Results validation

Intra-observer variability was assessed. An ANOVA test comparing both sets of measurements for each indicator (cIMT and cLD) indicated that there were no statistically significant differences ($p = 0.77$ and $p = 0.62$ respectively). The coefficients of variation were also calculated (1.8% for cIMT and 2.1% for cLD).

Table 2 provides the time spent on measuring as well as the number of points placed with each method.

Cimtool yielded good results on real images, some of which were of low quality and/or showed atherosclerotic plaque (see Fig. 7).

DISCUSSION

A thorough statistical analysis proved that the interactive measurement tool described in this work, Cimtool, can accurately measure the major indicator of cardiovascular risk (cIMT) and a stenosis indicator widely accepted in the literature (cLD). It is important to remark that cLD measured from a B-mode ultrasound image such as in this study is not sufficient to diagnose the grade of stenosis; it should be combined with a Doppler flow study for a correct assessment (Naylor et al. 2018). Moreover, a recent work indicated that the mean value of cLD for the population in this study corresponded to a healthy individual

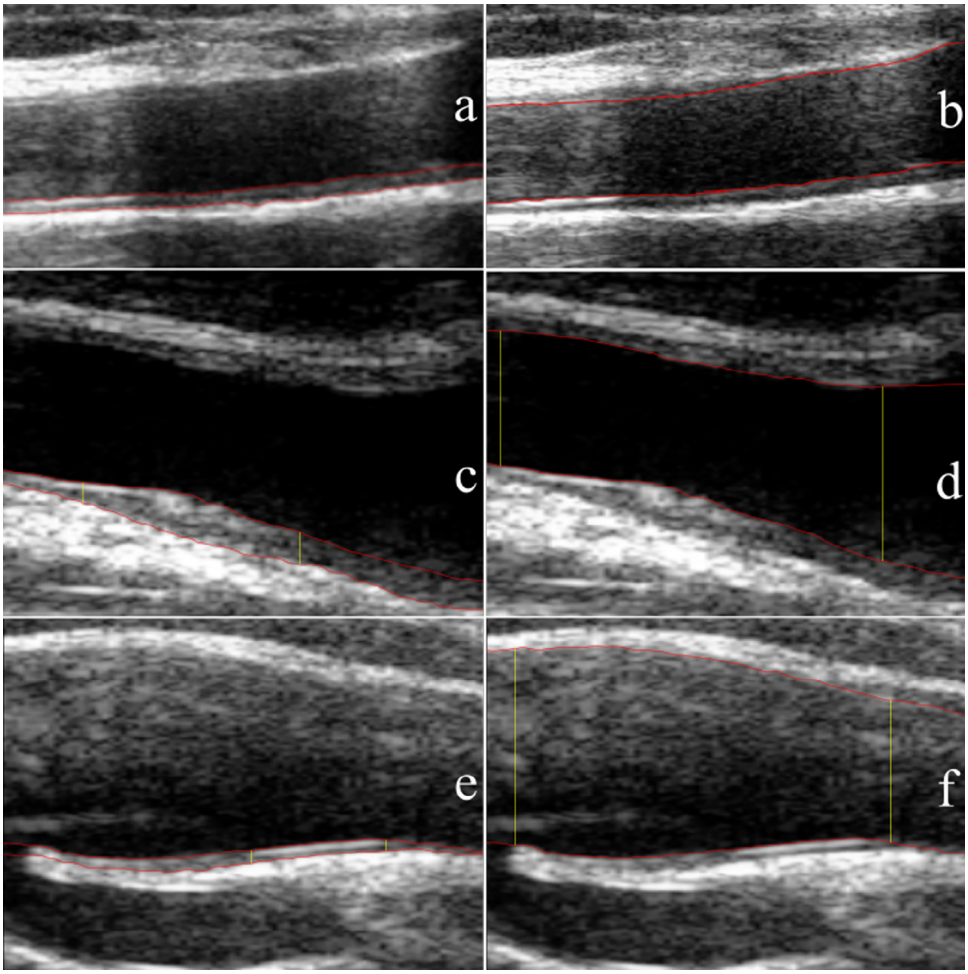

Fig. 7. Use of Cimtool in measuring real images reveals (a, c, e) contours over the far lumen–intima and intima–media interfaces (cIMT) and (b, d, f) contours over the near and far lumen–intima interfaces (cLD).

in the context of an epidemiological study (Diaz et al. 2017).

Analysis of Figures 2 and 5 reveals that the measurement workflow for each image with Cimtool is easier than in the manual method. For the latter, the expert places as many points as possible every time while taking care that they are in line with the corresponding points in the other interface to ensure a meaningful measurement.

The strong agreement with expert manual measurements indicates that Cimtool can be used to measure either cLD or cIMT. The active contour approach was especially useful because it provides more control over detection of the interfaces, especially when unclear or noisy boundaries are present. Automatic detection approaches can sometimes present problems (Bastida-Jumilla et al. 2013; Nicolaides et al. 2011; Saba et al. 2014; Sanchez et al. 2012), which occur frequently when using low-cost ultrasound equipment or probes (see Fig. 7).

Cimtool allows computation of far more measurements in less time and with lower standard deviation than the manual method (Table 1). An intra-observer evaluation of Cimtool indicated its strong reliability based on an ANOVA test performed over two sets of measurements. The coefficients of variation for the measurements and intra-observer variability were lower than those reported by Ring et al. (2016) and Araki et al. (2016). Also, expert users spend considerably less time using Cimtool compared with the manual method (Table 2).

Current results suggest that Cimtool can be used for assessment of real carotid ultrasound images (Fig. 7). Provided a data set, it can also be used to characterize a population according to cIMT or cLD, for the early detection and preventive treatment of cardiovascular events.

Cimtool is open source and can be used on a standard computer. It is freely available online, unlike most applications for cIMT and cLD measurement, facilitating research based on this software as well as its use by any physician or sonographer. Cimtool can be run as a MATLAB script, or it can be compiled to run as an application on any operative system.

CONCLUSIONS

An interactive tool (Cimtool) for measuring carotid intima–media thickness and carotid lumen diameter was developed. Those two indicators are the most accepted biomarkers for cardiovascular event risk and carotid stenosis assessment, respectively. Cimtool is based on an active contour scheme that allows the user to easily determine whether an interface detection is satisfactory or not. Cimtool was statistically validated using purposely developed carotid-like phantoms and real images, and measurements obtained with Cimtool were found to agree strongly with manual measurements and to have noise robustness. An Intra-observer analysis revealed reliability and repeatability between measurements. Our software is open source and it is available for free.

Acknowledgments—This project is partly funded by PICT 2014-1730 and PICT 2016-0116-FONCYT-ANPCYT of Argentina. H. L. Manterola and L. Lo Vercio are supported by a Consejo Nacional de Investigaciones Científicas y Técnicas (CONICET) Ph.D. grant. The financial support of these institutions is greatly appreciated.

The authors thank Mg. C. Marinelli from the Instituto Multidisciplinario sobre Ecosistemas y Desarrollo Sustentable at Universidad Nacional del Centro de la Provincia de Buenos Aires for support of and assistance with the statistical analysis of data.

REFERENCES

Araki T, Ikeda N, Molinari F, Dey N, Acharjee S, Saba L, Suri J. Link between automated coronary calcium volumes from intravascular ultrasound to automated carotid IMT from B-mode ultrasound in coronary artery disease population. Int Angiol 2014;33:392–403.

Araki T, Ikeda N, Dey N, Acharjee S, Molinari F, Saba L, Godia EC, Nicolaides A, Suri JS. Shape-based approach for coronary calcium lesion volume measurement on intravascular ultrasound imaging and its association with carotid intima-media thickness. J Ultrasound Med 2015;34:469–482.

Araki T, Kumar AM, Krishna Kumar P, Gupta A, Saba L, Rajan J, Lavra F, Sharma AM, Shafique S, Nicolaides A, Laird J, Suri J. Ultrasound-based automated carotid lumen diameter/stenosis measurement and its validation system. J Vasc Ultrasound 2016;40:120–134.

Avezum Á, Braga J, Santos IS, Guimarães HP, Marin-Neto JA, Piegas LS. Cardiovascular disease in South America: Current staabrera Fischer E. Carotid intima media thickness referencetus and opportunities for prevention. Heart 2009;95:1475–1482.

Bastida-Jumilla MC, Menchón-Lara RM, Morales-Sánchez J, Verdú-Monedero R, Larrey-Ruiz J, Sancho-Gómez JL. Segmentation of the common carotid artery walls based on a frequency implementation of active contours. J Digit Imaging 2013;26:129–139.

Bastida-Jumilla MC, Menchón-Lara RM, Morales-Sánchez J, Verdú-Monedero R, Larrey-Ruiz J, Sancho-Gómez JL. Frequency-domain active contours solution to evaluate intima–media thickness of the common carotid artery. Biomed Signal Process Control 2015;16:68–79.

Bots ML, Baldassarre D, Simon A, De Groot E, O'Leary DH, Riley W, Kastelein JJ, Grobbee DE. Carotid intima-media thickness and coronary atherosclerosis: Weak or strong relations? Eur Heart J 2007;28:398–406.

Delsanto S, Molinari F, Giustetto P, Liboni W, Badalamenti S, Suri JS. Characterization of a completely user-independent algorithm for carotid artery segmentation in 2-D ultrasound images. IEEE Trans Instrum Meas 2007;56:1265–1274.

Diaz A, Bia D, Zócalo Y, Manterola H, Larrabide I, Lo Vercio L, del Fresno M, Cabrera Fischer E. Carotid intima–media thickness reference intervals for a healthy argentinean population aged 11–81 years. Int J Hypertens 2017;8086714.

Golemati S, Stoitsis J, Sifakis EG, Balkizas T, Nikita KS. Using the hough transform to segment ultrasound images of longitudinal and transverse sections of the carotid artery. Ultrasound Med Biol 2007;33:1918–1932.

Ikeda N, Kogame N, Iijima R, Nakamura M, Sugi K. Impact of carotid artery ultrasound and ankle-brachial index on prediction of severity of syntax score. Circ J 2013;77:712–716.

Ikeda N, Gupta A, Dey N, Bose S, Shafique S, Arak T, Godia EC, Saba L, Laird JR, Nicolaides A, Suri J. Improved correlation between carotid and coronary atherosclerosis syntax score using automated ultrasound carotid bulb plaque IMT measurement. Ultrasound Med Biol 2015;41:1247–1262.

Lo Vercio L, Orlando JI, del Fresno M, Larrabide I. Assessment of image features for vessel wall segmentation in intravascular ultrasound images. Int J Comput Assist Radiol Surg 2016;11:1397–1407.

Manterola HL, Lo Vercio L, Díaz A, Pardini PA, Waks Serra MV, del Fresno M, Larrabide I. Low-cost phantoms for validating measurements in ultrasound vascular images; 2017. Proc SPIE 12th International Symposium on Medical Information Processing and Analysis. 10160.

McCloskey K, Ponsonby AL, Carlin JB, Jachno K, Cheung M, Skilton MR, Koleff J, Vuillermin P, Burgner D. Reproducibility of aortic intima–media thickness in infants using edge-detection software and manual caliper measurements. Cardiovasc Ultrasound 2014;12:18.

McInerney T, Terzopoulos D. Deformable models in medical image analysis: a survey. Med Image Anal 1996;1:91–108.

Molinari F, Zeng G, Suri JS. A state of the art review on intima–media thickness (IMT) measurement and wall segmentation techniques for carotid ultrasound. Comput Methods Programs Biomed 2010;100: 201–221.

Naylor A, Ricco JB, de Borst G, Debus S, de Haro J, Halliday A, Hamilton G, Kakisis J, Kakkos S, Lepidi S, Markus H, McCabe D, Roy J, Sillesen H, van den Berg F, Kohl P, Chafke N, Hinchliffe R, Koncar I, Lindholt J, Vega de Ceniga F, Verzini F, Archie J, Bellmunt S, Chaudhuri A, Koelemay M, Lindhal A, Padberg F, Venermo M. Management of atherosclerotic carotid and vertebral artery disease: 2017 clinical practice guidelines of the European Society for Vascular Surgery (ESVS). Eur J Vasc Endovasc Surg 2018;55:3–81.

Nicolaides A, Beach KW, Kyriacou E, Pattichis CS. Ultrasound and carotid bifurcation atherosclerosis. New York: Springer Science & Business Media; 2011.

Polak JF, Pencina MJ, Meisner A, Pencina KM, Brown LS, Wolf PA, D'Agostino RB. Associations of carotid artery intima-media thickness (IMT) with risk factors and prevalent cardiovascular disease. J Ultrasound Med 2010;29:1759–1768.

Pursnani S, Diener-West M, Sharrett AR. The effect of aging on the association between coronary heart disease risk factors and carotid intima media thickness: An analysis of the Atherosclerosis Risk in Communities (ARIC) cohort. Atherosclerosis 2014;233:441–446.

Ring M, Eriksson M, Jogestrand T, Caidahl K. Ultrasound measurements of carotid intima–media thickness by two semi-automated analysis systems. Clin Physiol Funct Imaging 2016;36:389–395.

Saba L, Sanches JM, Pedro LM, Suri JS. Multi-modality atherosclerosis imaging and diagnosis. New York: Springer; 2014.

Sanchez JM, Lanes AF, Suri JS. Ultrasound imaging. New York: Springer; 2012.

Shung KK. Diagnostic ultrasound: Imaging and blood flow measurements, 2nd ed. London: CRC Press; 2015.

Sobieszczyk P, Beckman J. Carotid artery disease. Circulation 2006; 114:244–247.

Suri JS, Yuan C, Wilson DL. Plaque imaging: pixel to molecular level, vol. 113. Amsterdam: IOS Press; 2005.

Touboul PJ, Hennerici M, Meairs S, Adams H, Amarenco P, Bornstein N, Csiba L, Desvarieux M, Ebrahim S, Hernandez Hernandez R, Jaff M, Kownator S, Naqvi T, Prati P, Rundek T, Sitzer M, Schminke U, Tardif J, Taylor A, Vicaut E, Woo K. Mannheim carotid intima-media thickness and plaque consensus (2004–2006–2011). Cerebrovasc Dis 2012;34:290–296.

Wikstrand JC. Methodological considerations of ultrasound measurement of carotid artery intima-media thickness and lumen diameter. In: Nicolaides A, Beach KW, Kyriacou E, Pattichis CS, (eds). Ultrasound and carotid bifurcation atherosclerosis. London: Springer-Verlag; 2011. p. 165–176.

World Health Organization (WHO). Noncommunicable diseases country profiles 2014. Geneva: Author; 2014. Available at: http://www.who.int/nmh/publications/ncd-profiles-2014/en/. Accessed September 1, 2017.

World Health Organization (WHO). World Health Organization Cardiovascular diseases; 2016. Fact sheets for cardiovascular diseases. Geneva: Author, 2016. Available at: http://www.who.int/gho/publications/world_health_statistics/2016/en/. Accessed September 1, 2017.